Supported ionic liquid membrane based on [bmim][PF_6] can be a promising separator to replace Nafion in microbial fuel cells and improve energy recovery: A comparative process evaluation

László Koók[1], Barbara Kaufer[1], Péter Bakonyi[1,*], Tamás Rózsenberszki[1], Isaac Rivera[2], Germán Buitrón[3], Katalin Bélafi-Bakó[1], Nándor Nemestóthy[1]

[1]Research Institute on Bioengineering, Membrane Technology and Energetics, University of Pannonia, Egyetem ut 10, 8200 Veszprém, Hungary

[2]Institute of Environmental and Sustainable Chemistry, TU-Braunschweig, Hagenring 30, 38106 Braunschweig, Germany

[3]Laboratory for Research on Advanced Processes for Water Treatment, Instituto de Ingeniería, Unidad Académica Juriquilla, Universidad Nacional Autónoma de México, Blvd. Juriquilla 3001, Querétaro 76230, Mexico

[*]Corresponding Author: Péter Bakonyi
Tel: +36 88 624385
E-mail: bakonyip@almos.uni-pannon.hu

Abstract

In this study, mixed culture bioelectrochemical systems were operated with various membrane separators: one prepared with 1-Butyl-3-methylimidazolium hexafluorophosphate ([bmim][PF_6]) ionic liquid and another one called Nafion, used as reference for comparative evaluation. In the course of experiments, the primary objective was to reveal the influence of membranes-type on microbial fuel cell (MFC) behavior by applying a range of characterization methods. These included cell polarization measurements, monitoring of dehydrogenase enzyme activity and cyclic voltammetry for the analysis of anode biofilm properties and related electron transfer mechanism. Additionally, MFC performances for both membranes were assessed based on Coulombic efficiency as well as substrate (acetate) concentration dependency of energy yields. As a result, it was demonstrated that the ionic liquid-containing membrane could be suitable to compete with Nafion and appears as a candidate to be further investigated for microbial electrochemical applications.

Keywords: microbial fuel cell; membrane; separator; ionic liquid; cyclic voltammetry; dehydrogenase enzyme activity

Notation list

MFC: microbial fuel cell

PEM: proton selective/exchange membrane

SILM: supported ionic liquid membrane

PEM-MFC: MFC equipped with Nafion 115 PEM

[bmim][PF_6]: 1-butyl-3-methylimidazoluim hexafluorophosphate ionic liquid

ILM-MFC: MFC equipped with SILM (containing [bmim][PF_6])

IL: ionic liquid

PVDF: polyvinylidene difluoride

DA: dehydrogenase enzyme activity [$\mu g\ mL^{-1}$ toluene]

CV: cyclic voltammetry

R_e: external resistor in the MFC electric circuit [Ω]

R_i: total internal resistance of MFC [Ω]

V: electric voltage [mV]

I: electric current [mA]

P: electric power [mW]

I_d: current density normalized to apparent anode surface area [$mA\ m^{-2}$]

P_d: power density normalized to apparent anode surface area [$mW\ m^{-2}$]

Y_S: specific energy yield (the electric energy recovered based on the COD added and apparent anode surface area [$kJ\ g_{COD,in}\ m^{-2}$]

CE: Coulombic efficiency [%]

TTC: 2,3,5-triphenyltetrazolium chloride

TF: triphenyl formazan

CDP: cell design point of MFC

OCV: open circuit voltage [mV]

E_a: anode electrode potential [mV]

E_c: cathode electrode potential [mV]

1. Introduction

Among microbial electrochemical systems, MFC technology is currently one of the most rapidly developing one, having the ability to transform the chemical energy (stored in various substrates) into the form of electricity by exploiting the metabolism of so-called exoelectrogenic microorganisms [1]. As it turned out from the research progress of the past years, not only simple compounds (including sugars, alcohols, volatile fatty acids, etc., used mostly in fundamental studies [2]), but also different complex, environmentally-threatening waste streams can be seen as suitable as feedstocks to operate the bioelectrochemical systems [3-8]. thus, MFCs show a good opportunity for the simultaneous management of pollutants and production of electrical energy [9].

So far, the widespread application of these biologically-assisted setups has not been typically realized at an industrial level, however, some successful implementations were communicated at real, scaled-up wastewater treatment plants [10, 11]. The reason behind this, as a matter of fact, can be associated with the notable number of existing challenges to be resolved so as to achieve cost-effective operation and decent performance [9, 12]. Some of the hurdles to overcome, besides microbiological aspects, are related to the MFC architecture [13]. Basically, from this point of view, MFCs are classified as single- and two-compartment devices, depending on the actual cell configuration and in particular how the electrodes (anode and cathode, serving as terminal electron acceptors and donors, respectively) are separated from each other [14].

In case of dual-chambered constructions, the physical separators, commonly membranes play a remarkable role (i.e. to maintain proton transfer from anode to cathode) and should therefore reflect traits such as (i) chemical stability, (ii) high ionic conductivity (or in other words, low membrane resistance) [15], (iii) appropriate selectivity for protons [16] and low permeability for oxygen (to defend the anaerobic conditions in the anode side)

[17]. In addition, the occurrence of pH splitting (the acidification of the anolyte and alkalination of catholyte due to the transport of cations other than protons) [18, 19], substrate cross-over and biofouling can also have significantly negative effect on the current generation capability and overall energy efficiency of MFCs. Hence, the development of membranes that fulfill these requirements and manage to counteract such technological issues are of interest.

As of now, PEMs are applied in most laboratory-scale MFC systems, first and foremost made of Nafion [20]. However, in this case, insufficient resistance to oxygen mass transfer and susceptibility of its sulfonate functional groups to be occupied by cations (e.g. Na^+ and K^+ instead of protons) can lead to remarkable decrease in MFC performance [21-23]. Recently, promising advancements have been observed in the literature studies employing alternative materials [24-31]. Among them, lately, membrane separators prepared with ILs have gained attention [32-34]. Previously, the potential of using certain SILM instead of Nafion was presented [33]. In a follow-up work [34], the comparative evaluation of such IL-based membrane separators was carried out, yielding useful feedback related to their oxygen and substrate (acetate) mass transfer properties. As a continuation of this research line (to deepen and further improve the knowledge), MFCs assembled with membranes containing [bmim][PF_6] ionic liquid were tested in the present work. The bioprocess was assessed via:

- monitoring biological adaptation by dehydrogenase enzyme activity
- running cyclic voltammetry (CV) to characterize the mechanism electron transfer
- conducting cell polarization to determine total internal resistances,
- performing electrochemical impedance spectroscopy (EIS) to evaluate the contribution of (i) charge transfer, (ii) electrolyte (membrane+solution) and implicitly the (iii) diffusion resistances.

It is believed that the outcomes delivered by this comprehensive (microbiological + electrochemical) approach can assist the better understanding of MFC behaviors (as a function of actual membrane type and characteristics) and in such a way, enrich the relevant literature with important/novel data.

2. Materials and Methods

2.1. Supported ionic liquid membrane (SILM) preparation

The SILMs were fabricated by immobilizing [bmim][PF_6] ionic liquid (IoLiTec, Germany) in the pores of hydrophobic Durapore PVDF microfiltration supporting membrane (Sigma-Aldrich, USA). The diameters of the PVDF membrane (116 μm mean thickness) and its micropores were 8 cm and 0.22 μm, respectively. 3 mL of [bmim][PF_6] was used for membrane preparation and before use, the membrane surface was gently cleaned to remove the excess ionic liquid as much as possible. Until use, the SILM was stored in sealed Petri-dish at room temperature (Some more information about the procedure can be found elsewhere in our previous papers i.e. [33]). As a result, the SILMs contained in average 20.5 mg cm^{-2} ionic liquid on basis of (support) membrane surface area. This value is in the same order of magnitude reported in our previous work [33] and also comparable to the those documented by Hernández-Fernández et al. [32] using various IL-based membrane separators in microbial fuel cells. The thickness of the prepared SILMs in contact with electrolytes (swollen-state) was 125 μm in average.

2.2. MFC setup

The two-chamber, batch MFCs used in this study were made of plexiglass and operated with a working volumes of 160 mL (both anode and cathode sides) (**Fig. 1**). The anode electrode with 26 cm^2 of apparent surface

area was carbon felt (Zoltek PX35, Zoltek Corp., USA), while in the aerated cathode chamber, carbon cloth (0.3 mg Pt cm^{-2}, FuelCellsEtc, USA) as cathode was used with apparent surface area of 8 cm^2. Both electrodes were connected to an external circuit through titanium wiring (Sigma-Aldrich, USA). To monitor the potential difference between the anode and cathode electrodes, the circuit comprised of 1 kΩ R_e (**Fig. 2A**), which was changed after two weeks of operation to 100 Ω (**Fig. 2B**) on the basis of polarization measurements (revealing the significant reduction of internal resistance to this order of magnitude). Phosphate buffer (50 mM, pH = 7) was used as catholyte solution in this study. At the beginning, (80 mL) activated sludge collected from the anaerobic pool of wastewater treatment plant (with pH adjusted to 7) was filled to the anode chamber for inoculation. Information about the microbial composition of the sludge can be found in our previous paper [35]. The rest of the anolyte was phosphate buffer with Na-acetate as carbon source [22]. Acetate was dosed repeatedly in different amounts to ensure the actually desired concentration (5 – 10 mM, **Fig. 2**). In each feeding cycles where the acetate solution was loaded, the equivalent volume of spent media was drawn before. Once the recorded voltage (closed-circuit potential difference between the electrodes) dropped close to the initial, consecutive feeding was applied to start the new experimental cycle.

The anode compartment was purged initially with nitrogen gas to remove dissolved oxygen content. The anode and cathode chambers were separated either by Nafion 115 PEM (Sigma-Aldrich, USA) or the SILM membrane, both cut to circle shape with 8 cm diameter. The Nafion membrane was pretreated before use as described by Ghasemi et al. [36]. The reactors were placed in an incubator and operated under constant mesophilic temperature of 35 °C. During CV measurements, an Ag/AgCl reference electrode (filled with 3 M KCl solution) was inserted to the anode chamber of the cells (more details on CV can be found in Section 2.3.4.).

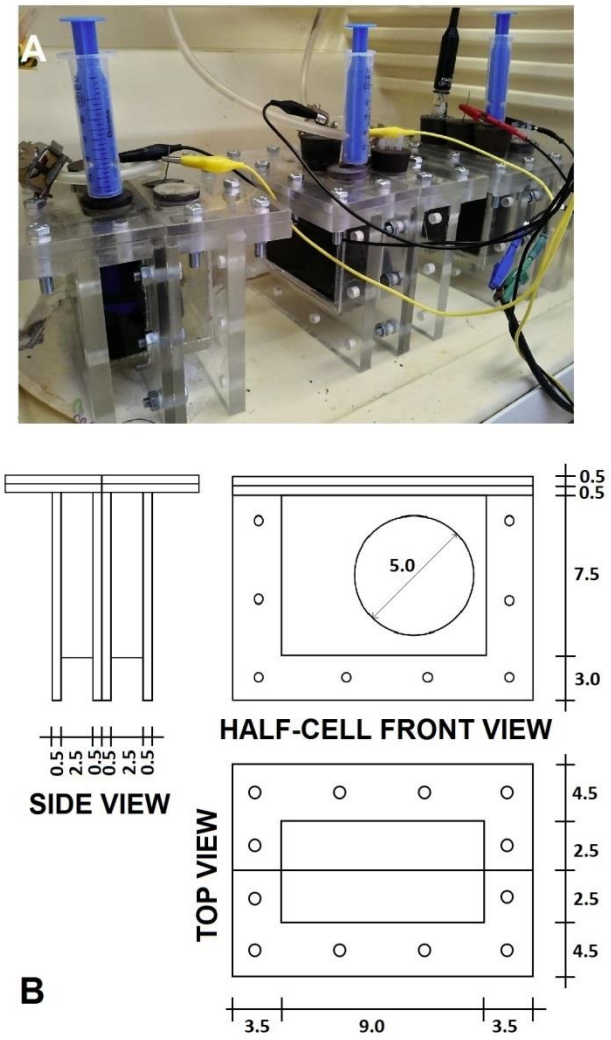

Fig. 1 – Image (A) and scheme (B) of the MFCs used in this study. Dimensioning is in cm.

2.3 Analysis and calculation

2.3.1. Calculations to report MFC efficiency

The cell voltage was continuously registered by using a data acquisition device (National Instruments, USA). *I* and *P* were calculated based on Ohm's law (considering the actual value of external resistor applied in the circuit, Section 2.2.). From these data, I_d *and* P_d could be derived. Y_S, describing the MFCs from the point of view of energy recovery, was computed by Eq. 1 [34]).

$$Y_S = \frac{\int_0^{\tau} P(t)dt}{m(COD_{in})\,A} \quad (1)$$

To evaluate charge utilization (reflected by the ratio of (i) the charge successfully recovered in form of electricity and (ii) the charge contained in the organic matter consumed), Coulombic efficiency was calculated according to Eq. 2 [1].

$$CE = \frac{M \int I\,dt}{\Delta COD\; F\; V\; b} \quad (2)$$

where M is the molar mass of oxygen (g mol^{-1}), ΔCOD is the change in chemical oxygen demand (g L^{-1}) during the process (COD was measured according to standard methods), F is the Faraday's constant (96485 C mol^{-1} electron), V is the total volume of the anolyte (L) and b is the number of electrons exchanged per 1 mol of O_2.

2.3.2. Statistical analysis

The statistical evaluation was carried out in Statistica 8 software to compare MFCs operated with Nafion and SILM based on t-test (**Table 1**), using the closed-circuit cell voltage data (as dependent variable), collected over time for each stages indicated in **Fig. 2**.

2.3.3. Dehydrogenase enzyme activity measurements

Dehydrogenase enzyme activity was estimated based on the reduction of TTC to TF [37]. In case of bulk samples, 1350 μl of Luria-Bertani medium was mixed with 300 μl sample taken from the anolyte. Then, 150 μl TTC reagent (5 g L^{-1}) was added to this mixture. In case of anodic samples, 2.2 x

0.5 x 0.2 cm pieces were cut off from the anode and put into the reaction mixture. After 20 min of stirring at 200 rpm, 12 hours long incubation period at 37 °C was ensured [38]. Prior to extraction of formed TF by stirring the mixture with 0.5 mL toluene at 200 rpm for 30 min, the reduction reaction was stopped by injecting 100 μl of cc. sulfuric acid. Thereafter, the mixture in the Eppendorf was centrifuged (4000 rpm, 5 min) and the toluene phase (supernatant) was subjected to absorbance measurement at 492 nm using UV-VIS spectrophotometer.

2.3.4. Electrochemical techniques

To derive fuel cell polarization curves, the external resistor was sequentially changed from 47 kΩ down to 10 Ω and the potential difference between anode and cathode electrodes was monitored after 20 min (provided to reach the stabilization of potential signal under each condition). From the linear range of the polarization curves (V vs. I) the value of R_i was determined based on the slope of the fitted trendline. In addition, the maximal P_d values were estimated considering the peak of the P_d vs. I_d plots.

CV was carried out by using a potentiostat (type: PalmSens 3, PalmSens, Netherlands) in a three-electrode arrangement, where the anode and cathode played the role of working and counter electrode, respectively, meanwhile an Ag/AgCl electrode (placed in the anode chamber and filled with 3 M KCl solution) was used as reference electrode. It is noteworthy that all electrode potential values reported in this paper are given with respect to Ag/AgCl (3 M KCl) reference electrode. CV measurements were conducted under non-turnover conditions at different stages of MFC operation (three times in each condition, accepting the third scan to be representative). The voltammograms were recorded by using 1 mV s^{-1} scan rate between +0.25 V and -0.65 V anode potentials (vs. Ag/AgCl, 3 M KCl), unless otherwise stated.

EIS measurements were carried out by using the impedance analysis function of the combined potentiostat (PalmSens 3, PalmSens, Netherlands) in

a whole-cell experimental setup (two-electrode arrangement), where the working electrode was the anode and the cathode served as both counter and reference electrodes. AC amplitude of 10 mV and frequency range of 50 kHz – 1 mHz were used. The measurements were conducted in presence of acetate substrate during the maximal electricity producing stage of the MFCs under open circuit operating mode (established two hours before EIS analysis). Equivalent circuit model fitting was carried out in EIS Spectrum Analyser software (ABC Chemistry).

3. Results and Discussion

3.1. Voltage profiles and current generation in response to different acetate supplementations

Once the cells were assembled, measurements and acquisition of data were started. During the acclimation period, varied amounts of acetate substrate were fed in subsequent batch cycles as indicated by arrows in **Fig. 2A**. After inoculation, as the start-up period commenced (no acetate feeding, **Fig. 2A**, first cycle), all MFCs showed quite low voltage outputs but the tendencies were different. On the one hand, almost prompt current generation was noted in case of PEM-MFC and after reaching a peak value, I_d remained around 51 mA m^{-2}. On the other hand, the ILM-MFC began to produce electricity less instantly (after a half-day) with a maximum I_d of about 63 mA m^{-2}. Overall, in this period, in accordance with the statistical analysis in **Table 1**, PEM-MFC generated significantly higher average voltages than ILM-MFC did (**Table 1**).

295 **Table 1 – Statistical analysis of voltages produced in MFCs operated with PEM and SILM**

Dependent variable: Closed-circuit voltage (mV)	Mean (PEM)	Mean (SILM)	t-value	df	p-value	Valid N (PEM)	Valid N (SILM)	Std. Dev. (PEM)	Std. Dev. (SILM)
no acetate feeding (Fig. 2A first cycle)	126.616	78.750	7.372	170	<0.001	86	86	16.383	57.939
5 mM acetate feeding (Fig. 2A second cycle)	223.354	191.196	5.355	214	<0.001	108	108	38.455	49.160
10 mM acetate feeding (Fig. 2A third cycle)	300.029	312.595	-2.416	520	0.016	261	261	71.549	44.043
5 mM acetate feeding (Fig. 2A fourth cycle)	241.715	277.429	-5.162	352	<0.001	177	177	60.960	68.974
7.5 mM acetate feeding (Fig. 2B first cycle)	85.459	107.727	-5.794	318	<0.001	177	143	20.008	46.044
5 mM acetate feeding (Fig. 2B second cycle)	61.190	97.097	-10.099	281	<0.001	140	143	20.424	36.898
6 mM acetate feeding (Fig. 2B third cycle)	66.252	108.159	-13.565	283	<0.001	149	136	8.166	36.735

$p < 0.05$ indicates statistical significance

positive t-value means that PEM performs better than SILM, while negative t-value presents the opposite case

After 2 days, the first dose of acetate was injected (**Fig. 2A**, second cycle) to ensure 5 mM concentration in the anode compartment. As a result, quick response could be observed after this organic matter loading in both systems. Still, the PEM-MFC reflected statistically higher voltages (**Table 1**), reaching 102 mA m^{-2} as highest current density. In the meantime, peak I_d of 88 mA m^{-2} was registered for the ILM-MFC. As it can be also seen in **Fig. 2A** (third cycle), the 10 mM acetate induced proportionally higher voltage and current density (compared to previous stage with 5 mM), peaking at 385 mV and corresponding 148 mA m^{-2} for PEM-MFC, whilst at 342 mV and 131 mA m^{-2} for ILM-MFC. It is noteworthy that in this period and onwards (**Table 1**), the ILM-MFC outperformed the PEM-MFC.

Moreover, it is important to notice the significantly different outcomes of the first and second 5 mM acetate additions (**Fig. 2A**, second and fourth cycles), which imply the proper and gradual development of the electrochemically-active populations. Actually, the extent of current density increase was clearly distinguishable for the reactors employing the two different separators. For instance, in case of MFCs equipped with PEM, the increment was nearly 30 % (133 mA m^{-2} vs. 102 mA m^{-2}), while for ILM-MFC, the 152 mA m^{-2} realized in the fourth cycle (**Fig. 2A**) represented a more than 72 % enhancement relative to the second cycle. Consequently, in this term, the bioelectrochemical system installed with SILM was capable to remarkably outperform its counterpart with Nafion.

As mentioned in Section 2.2., at the point of the 4^{th} substrate injection (**Fig. 2B**, first cycle), the external resistor was changed from 1 kΩ to 100 Ω in both ILM-MFC and PEM-MFC, because of the feedback received from cell polarization measurements (elaborated later on in Section 3.5.) indicating the change of total internal resistances over time. As a result, differences in the efficiency of the two systems became even more remarkable. In particular, as it can be seen in **Fig. 2B**, the highest voltages and thus, maximum current densities were considerably better for ILM-MFC, i.e. 739, 656 and 695 mA m^{-2}

compared to 461, 348 and 373 mA m^{-2} generated by PEM-MFC at 7.5, 5 and 6 mM acetate concentrations, respectively.

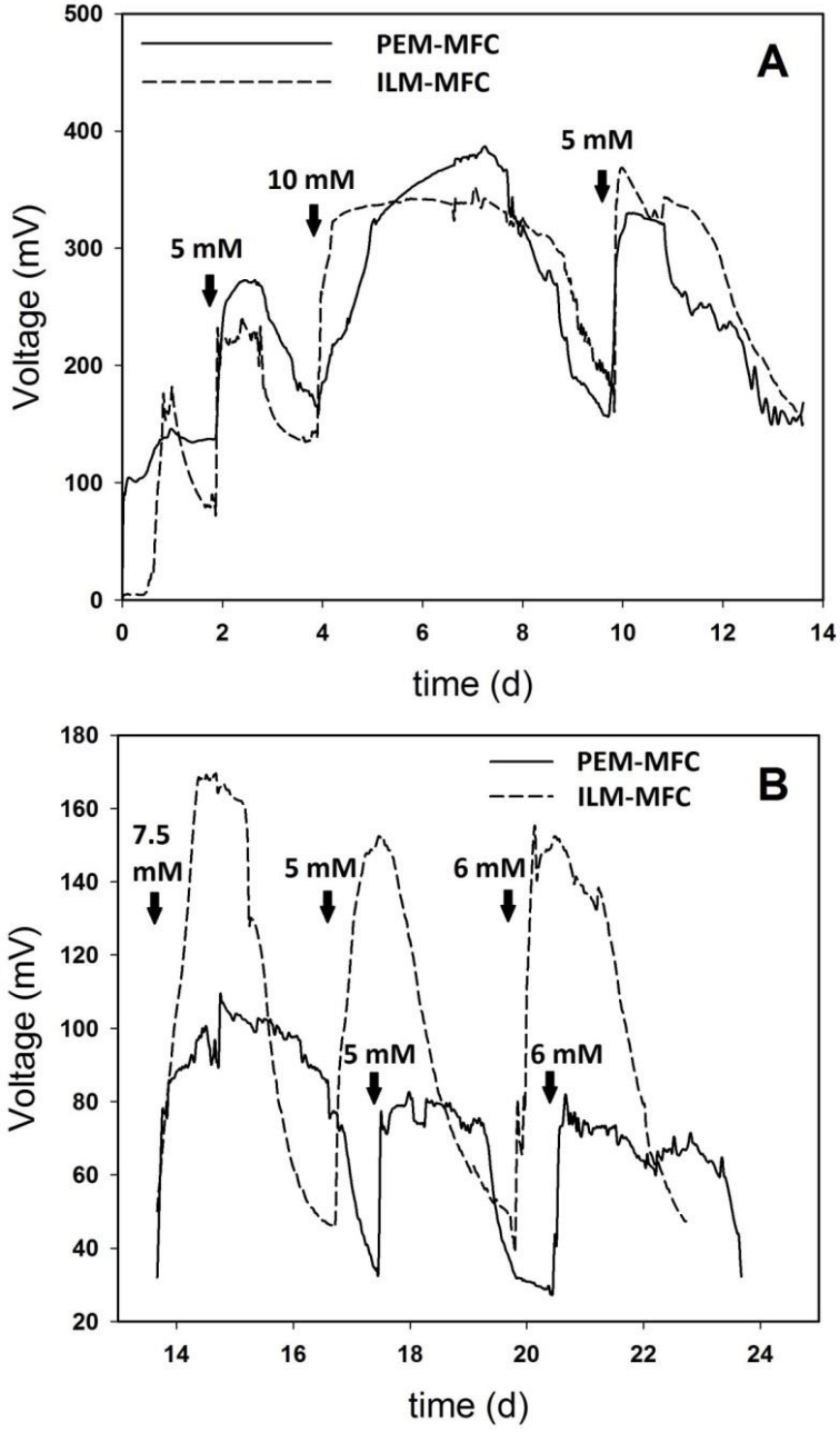

Fig. 2 – Voltage profiles of MFCs equipped with different membranes. Measurements at various acetate concentrations (A) R_i = 1 kΩ and (B) R_i = 100 Ω.

The total (cumulative) energy recovery (normalized to the anode surface area) is illustrated in **Fig. 3**. It can be seen that though PEM-MFC was more effective in generating electrical energy for the two initial feeding cycles (reflected also by the significantly higher, mean voltage values presented in **Table 2**), the ILM-MFC could take over with time (from the 3rd substrate addition and onwards) and perform in a considerably better way.

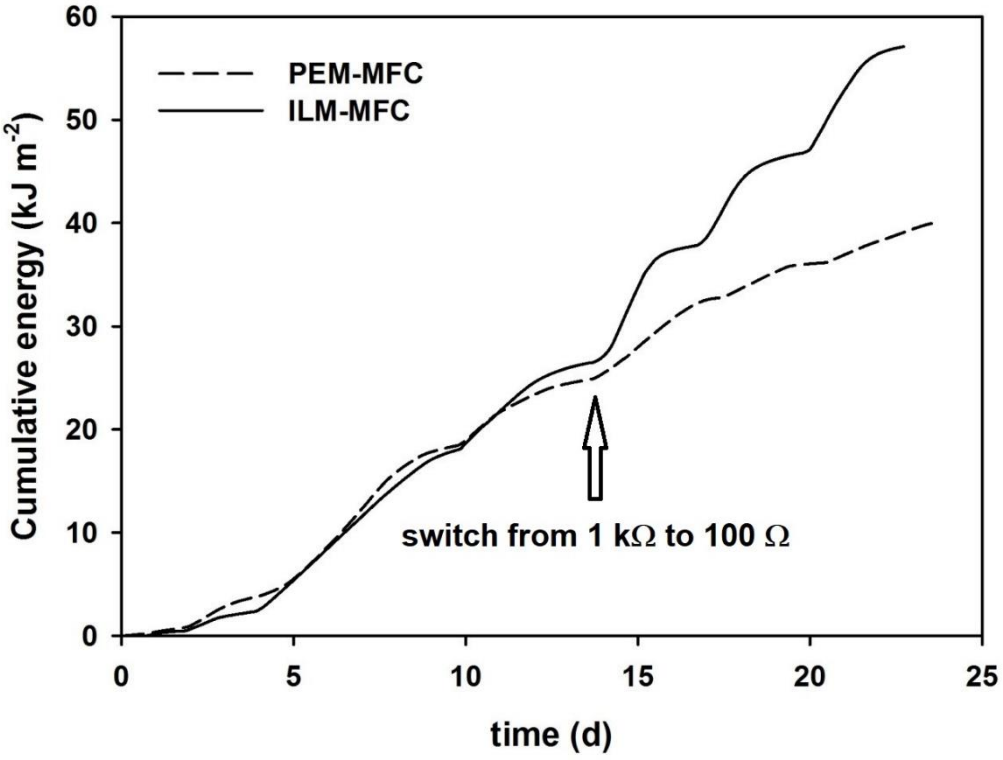

Fig. 3 – Cumulative energy production of MFCs equipped with different membranes under conditions displayed in **Fig. 2**.

At this point, besides the evaluation presented so far, we feel important to comment on process stability, which can be challenging when a supported ionic liquid membrane is used. In SILMs, the IL stays in the pores of supporting material thanks mainly to capillary forces, which is influenced by factors e.g. the viscosity of IL [39]. In addition, the compatibility of IL and the support membrane can affect consistent SILM performance as well as the formation of water microenvironments inside the IL phase [39].

In this aspect, as discussed by Fortunato et al. [40], the loss of immobilized liquid from the pores (in case of supported liquid membranes) can potentially be mitigated by the appropriate selection of the phase properties in contact, in particular the membrane and the solution around it. During SILM fabrication, for a given support matrix in which the IL is filled, the membrane traits can eventually be adjusted by the choice of IL, where the molecular structures of anion and cation (building up the IL) will play a significant role. If the purpose is the use of SILM in an aqueous media such as in MFCs (where anolyte as well as catholyte are water-based solutions) hydrophobic, room-temperature ILs may be more appropriate in order to reduce miscibility and consequently, the threat of possible leaching of IL from the membrane pores. In general, hydrophobicity of ILs with an imidazolium-type cation ($[C_nmim]^+$) increases with the length of alkyl side-chain and moreover, the anion ($[X]^-$) properties i.e. $[NTf_2]^-$ vs. $[PF_6]^-$ will also take an effect [41].

As a matter of fact, Fortunato et al. [42] investigated the durability of SILMs prepared with ILs of the imidazolium family i.e. [bmim][PF_6] and PVDF support membrane, similar to this study. In essence, it was reported that such SILMs could preserve their hydrophobic characteristic after contacted with water and furthermore, no considerable displacement of IL from the pores could be noted as long as mild stirring conditions were maintained. Additionally, in the continuation of that work [40], it was demonstrated that even if the concentration of imidazolium-type IL in the aqueous phase surrounding the SILM rose under dynamic (e.g. intensely stirred) circumstances, it was primarily originated from the rinsing of excess IL located on the membrane surface rather than from displacing the IL from the membrane pores.

On the grounds of these arguments and taking into account that no stirring was directly provided in the MFCs of this investigation – representing more or less static conditions on two, anode- and cathode-facing sides of the SILM (though continuous air supply in the cathode chamber may have had some inherent contribution here) – it may be supposed that SILMs

manufactured by embedding [bmim][PF_6] in microfiltration PVDF membrane could be considered stable enough. As a result, this SILM may be seen as a plausible candidate withstanding longer-term MFC operation, which is implied also by the outcomes of 3-4 weeks of experimentation lacking any membrane-associated failures (**Fig. 2**). Nevertheless, to strengthen these assumptions and conclusions, a future study can be proposed.

A further investigation on SILM stability and application can be also useful to take a look into process safety. On the one hand, from previous studies such as Nemestóthy et al. [43], it seems that ILs might act as inhibitors in anaerobic fermentation systems, depending on the IL type and concentration. Therefore, if leakage of ILs from the SILM occurs over time, it may cause challenges to keep the electro-active bacteria in good conditions and maintain sufficient process performance. However, this aspect should be examined case-specifically for the actual underlying microbial community, which, thanks to the wide range of inocula used by researchers, can be quite different from one MFC to another. On the other hand, nevertheless, Jebur et al. [44] have found that membranes prepared with ionic liquid can have anti-microbial impact and in that way, suppress the undesired biofouling of the separator. Such a property could deserve attention since fouling of membranes in bioelectrochemical systems can lead to severe operational issues.

3.2. Evaluation of bioelectrochemical cell performance applying ionic liquid-containing and Nafion membrane separators

The efficiency parameters (for instance substrate removal, Coulombic efficiency, energy yield, etc.) of microbial electrochemical systems are usually dependent on the operating conditions [1, 13], among which substrate concentration is one of the most important [45]. For instance, it has been previously found that ILM-MFCs were able to reach higher energy yields at low acetate concentrations than those relying on Nafion [33]. Hence, besides the

411 acetate loadings tested and discussed in Section 3.1., complementary
412 measurements along with additional substrate concentrations were carried out
413 and the dependency of Y_S on this process variable was assessed in MFCs
414 employing SILM or Nafion membrane. Overall, the 6 initial acetate
415 concentrations set in the anode chamber were as follows: 2, 5, 6, 7.5, 10 and
416 12 mM.

417 The results are illustrated in **Fig. 4**, where it is to observe that the energy
418 yield values were significantly enhanced between 2 – 7.5 mM substrate
419 concentrations (approximately 4x, 3x, 2.6x and 1.4x higher for 2, 5, 6 and 7.5
420 mM acetate, respectively) in case of ILM-MFC compared to PEM-MFC. At
421 higher acetate concentrations (10 and 7.5 mM), the differences between the
422 two cells became much smaller, but Y_S was still somewhat higher for the ILM-
423 MFC. This may suggest that under such substrate loadings, the metabolic
424 (substrate-utilizing) capacity of exoelectrogenic microorganisms in both MFCs
425 reached an upper-bound. Besides, the potential presence of methanogenic
426 *archaea* (occurring in the mesophilic, anaerobic sludge applied for inoculation)
427 should be also taken into account. This could affect the total energy recovery
428 via microbiological competition for the organic matter. This phenomenon can
429 be a possible threat at increased substrate availability [46].

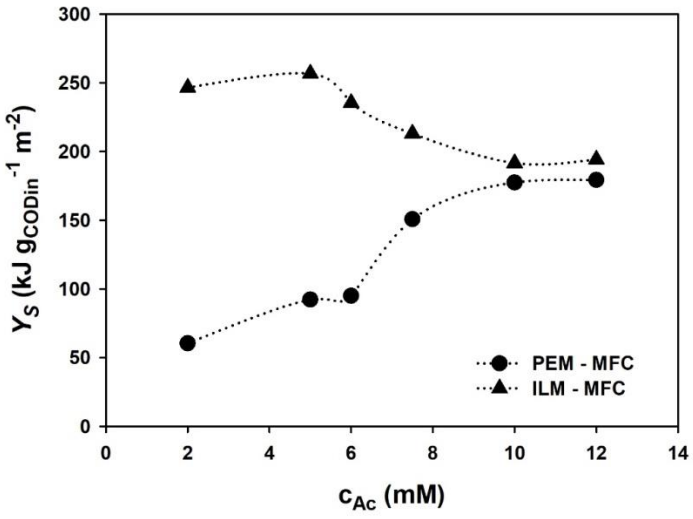

430

431 **Fig. 4** – Y_S as a function of acetate concentration. c_{Ac} represents initial acetate
432 concentrations in the anode chamber.

The largest Y_S was realized in the ILM-MFC (Y_S = 256.8 kJ $g_{COD,in}^{-1}$ m^{-2} at 5 mM acetate concentration), while 180 kJ $g_{COD,in}^{-1}$ m^{-2} could be achieved in the MFC using the Nafion proton exchange membrane (at 12 mM acetate concentration).

To evaluate the utilization of electrons (released from organic matter degradation) in MFCs, the Coulombic efficiency was determined at 6 mM acetate addition (last cycle in **Fig. 2B**). In fact, CE of 13.9 ± 0.4 % and 24.0 ± 0.7 % could be attained for the PEM-MFC and ILM-MFC, respectively. Therefore, from this point of view, the application of SILM resulted in a more attractive bioelectrochemical process. As for the alteration of CE in the function of substrate concentration, a decreasing tendency was presented by Sleutels et al. [47] within an acetate influent concentration range of 1 – 35 mM. This is in good agreement with the findings of our previous [33] and present studies, suggesting the use of low acetate concentrations in order to support higher specific energy recoveries (**Fig. 4**).

In summary, the experiments revealed the positive impact of SILM on both energy yield (especially at low substrate concentrations) and Coulombic efficiency. In addition, it turned out that the hydrophobic [bmim][PF_6]-based SILM can be used properly for separating the electrode chambers in two-compartment MFCs to produce electricity with an effectiveness more or less comparable to Nafion when higher substrate loadings are applied. Nevertheless, to dissect the possible contribution of membranes in the MFC' behaviors and facilitate the understanding of the process, further tests e.g. (i) cell polarization, (ii) monitoring of dehydrogenase enzyme activity as well as (iii) cyclic voltammetry were performed and are discussed in the next sections.

3.3. Analysis of MFC behavior via polarization measurements

The cell polarization measurements assist the calculation of R_i for MFCs and hence, help the selection of appropriate R_e by which P_d is enhanced. Under the condition then $R_i = R_e$, the CDP of MFC is reached [48].

On the third day after inoculation, R_i values were found to be 581 ± 11 Ω and 789 ± 9 Ω for ILM-MFC and PEM-MFC, respectively. Besides, estimated power densities at CDP were 39.8 ± 2.7 mW m^{-2} and 78.0 ± 3.1 mW m^{-2}, respectively. After two weeks, R_i values decreased considerably in both systems to 276 ± 16 Ω and 303 ± 11 Ω, respectively. The approximate maximum power densities at CDP were as high as 190.1 ± 9 mW m^{-2} and 98.6 ± 11.6 mW m^{-2} in case of ILM-MFC and PEM-MFC. The observed tendency during the first 14 days for R_i supports the conclusions of Section 3.1. pertain to the development of the MFCs reflected by current density outputs. Polarization measurements were continued and after three weeks, almost no additional change of R_i (268 ± 11 Ω and 302 ± 17 Ω for ILM-MFC and PEM-MFC, respectively) could be noted. Consequently, stabilization of maximal power densities was attained and the microbial fuel cells were considered as adapted systems (**Fig. 5**).

Basically, the characteristics of polarization (**Fig. 5**) curves are similar to those found in the relevant literature [23, 34, 49], showing a declining pattern in current density along with increased R_e. Furthermore, the absence of power overshoot is good indication of appropriate bioelectrochemical system operation [17]. Moreover, it is to infer that the MFCs employing the SILM not only achieved lower R_i but at the same time, ensured > 70 % higher maximal power density (500 ± 21 mA m^{-2} of I_d vs. 290 ± 19 mA m^{-2} for PEM-MFC) at CDP. The maximal 950 ± 84 mA m^{-2} of I_d (vs. 405 ± 30 mA m^{-2} for PEM-MFC) was accomplished with the lowest resistance (10 Ω), presumably because of effective electron discharge [49].

In this polarization study, voltage drop was more significant for PEM-MFC within the concentration polarization range (at high current density). It is a probable signal of more pronounced increase in the ratio of oxidized and reduced charge-shuttling molecules (being at different redox state) in the vicinity of electrode surface [1]. This assumed phenomena can be ascribed to the limited discharge of reduced or supply of oxidized compounds, leading to higher anode potentials or on the contrary, lower potentials at the cathode [1].

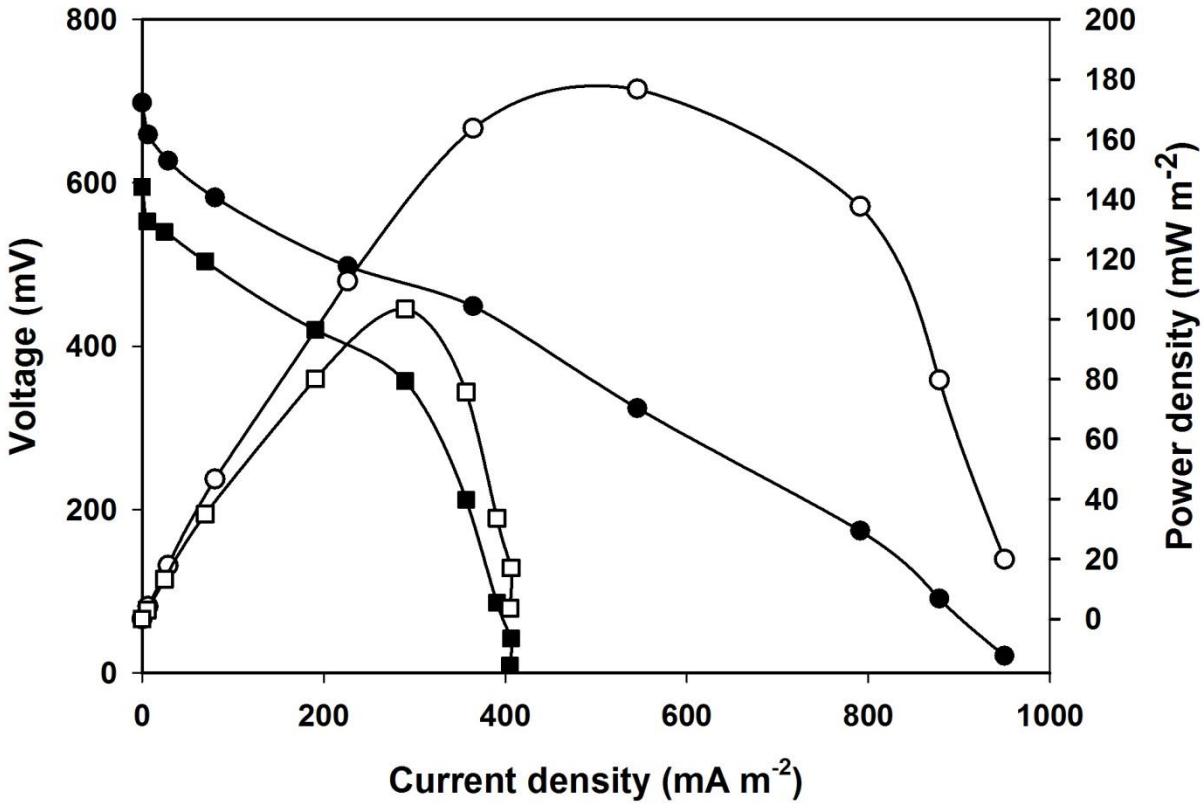

Fig. 5 – Polarization curves for (●) ILM-MFC and (■) PEM-MFC and power density plots for (○) ILM-MFC and (□) PEM-MFC (taken on the 21st day, 6 mM acetate)

It is important to mention that the attractiveness of membranes for MFCs should be assessed under the similar settings/combination of environmental factors [17] such as in terms of seed source, substrate quality, electrode materials, anode/cathode potential(s) and spacing, anolyte/catholyte solution traits i.e. conductivity, physiological conditions i.e. temperature, pH, etc. otherwise, it is difficult to say which system and in particular, which membrane is more suitable than another [50]. Nonetheless, in general, MFCs are capable of producing power densities both above and below the values reported in the present work (**Table 2**). Similar conclusions can be made on the grounds of the analysis carried out by Ge et al. [51], where it was clearly reported that

MFC power densities can span a wide range (through order of magnitudes), fitting our results obtained both with the IL-containing and Nafion membranes.

Table 2 – Comparative table with literature data. The power density data marked with (*) are given as granular anode volume specific values

MFC type	Membrane	Power density (mW m^{-2} / mW m^{-3*})	Internal resistance (Ω)	Substrate	Reference
Dual-chamber MFC	Nafion (3.5, 6.2 and 30.6 cm^2)	44 - 173	1110 – 89.2	Acetate	[23]
Dual-chamber MFC	Nafion (~20 cm^2)	51 – 67.5	300 - 500	Synthetic wastewater	[53]
Single-chamber MFC	[omim][PF_6]-PVC	45*	4500 – 5900	Brewery wastewater	[54]
	[mtoa][Cl]-PVC	450*	440 - 750		
Dual-chamber MFC	Nafion	100*	2000	Acetate	[34]
	[hmim][PF_6]	3.7	2900		
	[bmim][NTf_2]	3.9	2500		
	Nafion	12.2	1350		
Dual-chamber MFC	[bmim][PF_6]	179	268	Acetate	This study
	Nafion	101	302		

3.4. Alteration of electrode potentials in MFCs equipped with SILM or Nafion membrane

By monitoring both the individual anode and cathode potentials (and the difference between those values), information about the potential losses occurring in the system can be extracted and beside, the assignment of these losses to given processes (e. g. electrode reaction or diffusive transport, etc.) may be possible.

Considering the OCV of MFCs during acetate utilization (**Fig. 6A**), a strictly monotonic increase could be observed as a function of elapsed time in case of ILM-MFC, from 405 mV (on 3rd day) up to 698 mV (on 21st day). For PEM-MFC, however, such a trend could not be detected and rather, a nearly steady OCV (around 583 mV) was obtained. The determination of accompanying anode and cathode potentials revealed quite comparable values in the two systems: E_a = –452 ± 5 mV and E_a = –485 ± 25 mV in case of ILM-MFC and PEM-MFC, respectively. Nevertheless, the alteration of E_c with time in the two MFCs (assembled with various membrane separators) was more distinguishable. In ILM-MFC, change of E_c followed a similar pattern than respective OCV (**Fig. 6B**), resulting in an increment from +28 mV (3rd day) to +250 mV (on 21st day). As for PEM-MFC, E_c was found to be relatively higher at the early stage of operation (E_c = +79 mV, 3rd day) and rose to +120 mV on the 7th day. From that point onwards (14th and 21st days in **Fig. 6B**), a stabilized value (+93 ± 2 mV) could be measured.

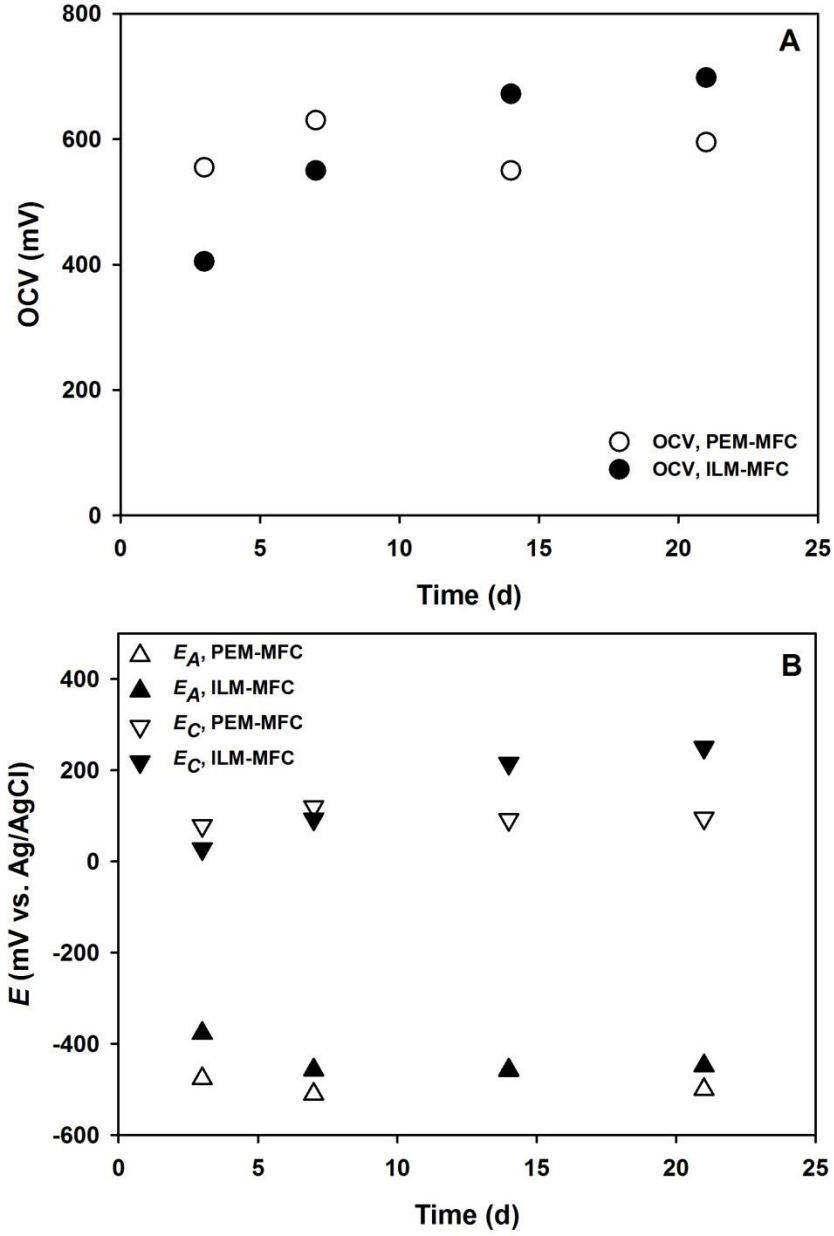

Fig. 6 – OCV (A) and electrode potentials (B) of the MFCs measured at maximal current density stages.

These phenomena imply the importance of the membrane separator type, which seemed to be a responsible factor for the registered changes of electrode potentials, in particular E_c. As a matter of fact, the transport of certain cations (e.g. Na^+ and K^+) may affect the migration of protons from the anode to the cathode, causing potentially a pH split due to H^+ accumulation in the anode chamber [19]. Hence, the passage of those ions through the

membrane presents an issue to deal with and can be associated with structural properties of the membrane material [19] since, for instance, the sulfonate groups of Nafion can get occupied by the above mentioned cationic species [21, 55, 56]. Additionally, problems related with the time-stability i.e. due to (bio)fouling of Nafion may arise [57]. In contrast, the SILM (based on [bmim][PF_6] ionic liquid and PVDF as supporting membrane layer, which would appear as a feasible separator candidate to improve (i) energy yields, (ii) current and power densities and (iii) lower cathodic losses – has several underexplored characteristics at the moment, including mechanism of H^+ transport and selectivity to transfer various compounds in the anolyte and catholyte (cross-over effect). In the light of that, the mechanism of ion transfer through ILs having special physico-chemical properties is one crucial aspect to be elaborated and compared to polymer membranes such as Nafion. Nonetheless, as it has been recently communicated in our previous paper [34], the SILMs can have lower O_2 mass transfer coefficients and one order of magnitude lower transport rate for acetate ion (referred as substrate cross-over), which can be another relevant information to take into account from a process evaluation point of view.

3.5. Assessment of SILM- and Nafion-dependent MFC behaviors by dehydrogenase activity monitoring

To further elucidate the observed differences in the behavior of MFCs assembled with various membrane separators, feedback from a biological activity viewpoint can be useful (i.e. the production of charge carriers is primarily attached to strain metabolism) [58]. Measurements on dehydrogenase enzyme are able to characterize the metabolism-related microbial redox activity, since this intracellular biocatalyst plays an important role on H^+ (and coupled e^-) transfer between metabolites and indirectly (by ensuring accessible charges and using redox mediators) on the maintenance of electron driving force [38].

In our system, samples taken from the bulk phase as well as from the anode (biofilm) were analyzed according to Section 2.3.3. In the former case, for both ILM-MFC and PEM-MFC, a progressively decreasing tendency was shown as the systems approached stable operation (**Table 3**).

Table 3 – Results of dehydrogenase activity measurements of bulk samples taken at different stages of system development

	DA ($\mu g\ mL^{-1}$ of toluene)	
	PEM-MFC	ILM-MFC
Day 3	20.77	15.8
Day 7	4.07	8.15
Day 21	2.82	3.27

This could be an indicator of lowered metabolic redox activity in the liquid surrounding the anode electrode [38]. This seems to be reasonable since in an MFC system, the proper development of an electro-active biofilm on the anode surface should be accompanied by the suppression of planktonic cells [59]. These results coincide well with the literature, where, for instance, DA over time was investigated by Reddy et al. [38] in single chamber MFCs at different organic loading rates. In brief, initial increase from 9 up to 18 $\mu g\ mL^{-1}$ toluene (until ~ 12^{th} hour) and a consecutive decrease down to 2 – 4 $\mu g\ mL^{-1}$ toluene were demonstrated for samples withdrawn from the anolyte (containing the suspended/planktonic cells).

In contrast, higher DA could be presumed in case of anodic samples because of the enrichment of active, anodophylic strains and indeed, supporting experimental results were obtained (**Table 3**). On the 3^{rd} day, the anodic DA values were somewhat similar, i.e. 1.23 $\mu g\ mL^{-1}$ toluene and 1.15 $\mu g\ mL^{-1}$ toluene for the PEM-MFC and ILM-MFC, respectively. Later on (in

parallel with the evolution of current described in Section 3.1.), the DA data (in both MFC systems) reflected rising tendencies with time. In case of ILM-MFC, values determined on the 7th and 21st days were 5.77 μg mL^{-1} toluene and 8.04 μg mL^{-1} toluene. For PEM-MFC, respective DAs were found as 3.33 μg mL^{-1} toluene and 6.11 μg mL^{-1} toluene (**Table 4**).

Table 4 – Results of dehydrogenase activity measurements of anode samples taken at different stages of system development

	DA (μg mL^{-1} of toluene)	
	PEM-MFC	ILM-MFC
Day 3	1.23	1.15
Day 7	3.33	5.77
Day 14	3.84	7.02
Day 21	6.11	8.04

To evaluate the likely positive effect of SILM on anode-related DA compared to PEM-MFC (indicated by the differences in DA), various mass transport phenomena (that may affect the microbial redox metabolism) taking place across the membrane should be considered. In agreement with the statements made above, SILMs can have lower oxygen transfer rate relative to Nafion, as communicated in our recent work using [bmim][NTf$_2$] ionic liquid [34]. This property could be helpful to more successfully protect the anode chamber from oxygen gas penetration and therefore, maintain anoxic conditions. In MFCs, it is a requirement to keep the anaerobic (electrochemically-active) microbes in good conditions and prevent metabolic shifts, which may occur once terminal electron acceptors (such as oxygen) other than the anode material itself are available for cell respiration. In addition, SILMs (compared to Nafion) can have the potential to act as effective barriers and reduce substrate-related losses linked to cross-over effect [34]. Faster transport of substrate towards the cathode chamber may result in

relatively lowered anode-side substrate concentration, which may limit the redox activity of microorganisms. Mainly, this issue can occur at initially low substrate concentrations, which was the case of the present study.

3.6. Cyclic voltammetric analysis of MFCs operated with SILM and Nafion membranes

In general, as discussed in Section 3.5., DA gives insight to the metabolic redox activity of particular microbial communities i.e. those located and growing on the anode [38]. Nonetheless, in order to characterize the electrochemically-active population itself, cyclic voltammetry (CV) can be proposed [60, 61]. The cyclic voltammograms in **Figs. 7A and B** revealed several oxidation-reduction peaks in both ILM- and PEM-MFCs and furthermore, suggest the dynamic variation of electrocatalytic activity on anodes, irrespective of the membrane used. Actually, the increase of detected peak currents over time indicate (i) the enrichment of redox mediators and/or (ii) larger coverage of anode by proteins involved in the electron transfer process [62]. Notwithstanding, a comprehensive approach is required when it is aimed to fairly compare various bioelectrochemically active systems based on the quantification of the above-mentioned mediators and/or proteins taking part in the electron transfer due to the commonly occurring lack of information about the actual bacterial concentrations [61, 63]. This appears to be the case in our MFCs as certain conditions were not identical for example in terms of anolyte properties such as ion and cell concentrations, which can be associated with the employment of membranes and their mass transport features.

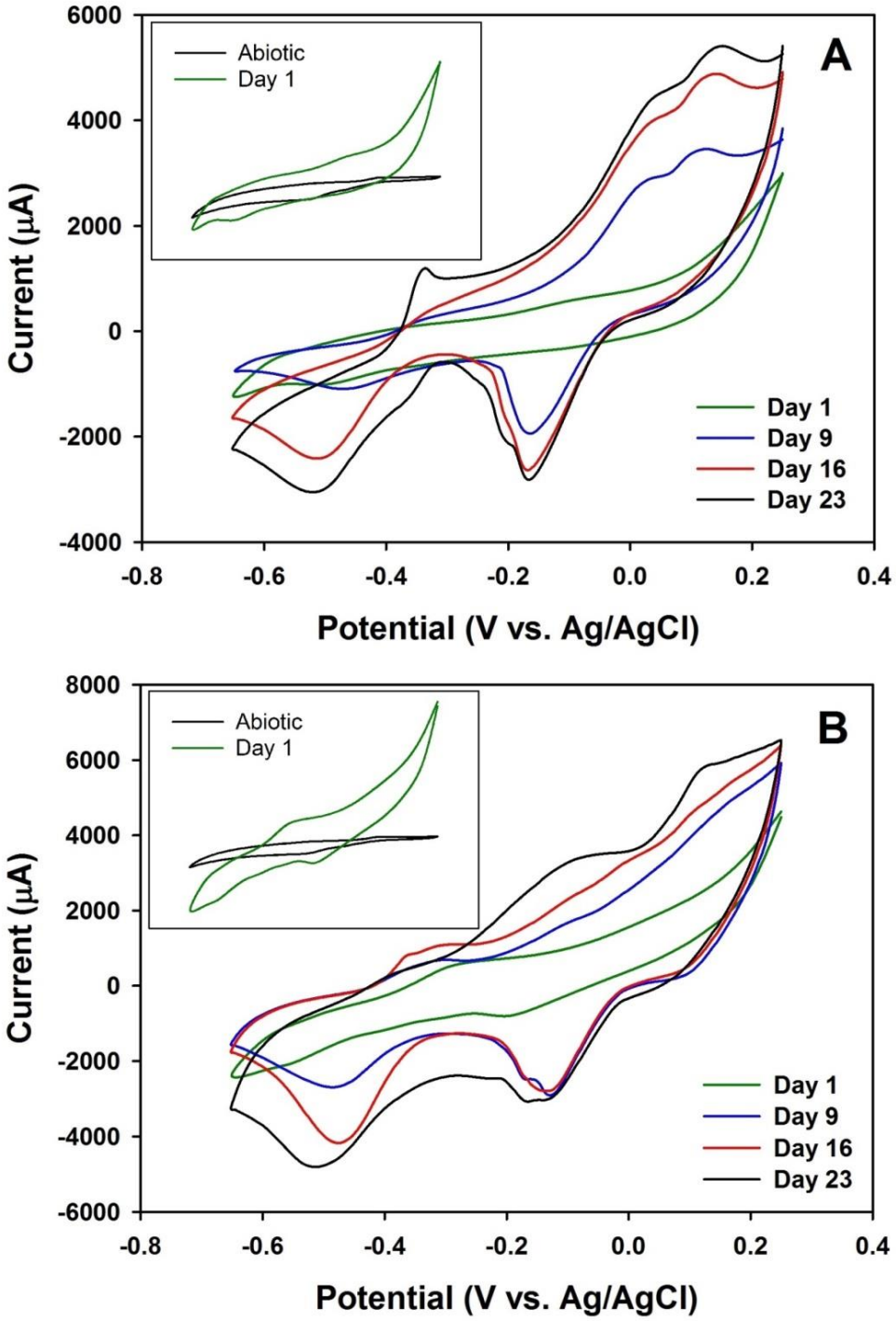

Fig. 7 – Cyclic voltammograms recorded at scan rate of 1 mV s^{-1} under non-turnover (under acetate substrate depleted).conditions: (A) ILM-MFC; (B) PEM-MFC.

Nonetheless, even under such conditions, the assessment of changes in each individual MFC can be performed. For instance, in **Fig. 7A**, a complex

redox behavior of ILM-MFC anode can be seen. The voltammogram (recorded on the 1st day) implied the existence of a weak reduction peak at –0.51 V (corresponding peak current: 1 mA) in the reverse scan, while no redox peaks could be detected for the virgin anode. After 9 days of operation, weak oxidation peaks were spotted at about (i) –0.35 V (corresponding peak current: 0.25 mA), (ii) +0.03 V (corresponding peak current: 2.8 mA) and (iii) +0.16 V (corresponding peak current: 3.5 mA) in the forward scan and at the same time, reduction peaks appeared at (iv) –0.18 V (corresponding peak current: 2 mA), (v) –0.47 V (corresponding peak current: 1mA) in the reverse direction. In accordance with **Fig. 7A**, it can be stated that the peak currents increased over time and moreover, on the 23rd day, two overlapping peaks were found at about –0.18 V and –0.2 V (3 mA and 2.1 mA). Overall, on the 23rd day, the anode of ILM-MFC could be characterized by (at least) three well-distinguishable redox systems.

Considering the CVs of PEM-MFC (**Fig. 7B**), no redox activity in case of virgin anode was observable, just like for ILM-MFC. Afterwards, on the 1st day, weak oxidation (–0.29 V) and reduction (–0.2 V) peaks appeared, with peak currents of about 0.3 mA and 1 mA, respectively. Similar to ILM-MFCs, the redox current peaks of the bioelectrochemical system equipped with Nafion membrane increased as a function of operation time, resulting also in (at least) three active redox components (**Fig. 7B**). In summary, slight differences could be identified in terms of the (i) oxidation peaks in the forward scan and (ii) the absolute values of peak currents, compared to ILM-MFC.

Thereafter, additional CV measurements were carried out by adjusting the scan rate in the following order to 50, 25, 20, 15, 10, 5, 1 mV s^{-1} so as to evaluate the dependency of peak current on the scan rate (data not shown). In essence, it could be observed that the peak current was proportional to the square root of scan rate, which implies diffusion limitations [65, 66]. Therefore, it is to assume that the electron transfer from the biofilm to the anode could have taken place via redox mediators [67], rather than through a direct connection established between the cell membrane-bound redox enzymes and

694 the terminal electron acceptor (anode). According to the peak shifting
695 phenomenon the systems could be considered as quasi-reversible with 'slow'
696 electron transfer process taking place [64]. Since the redox peak areas
697 increased simultaneously with the current generated (as described in Section
698 3.1.), it would appear that these electron-shuttling substances were secreted
699 by the electroactive bacteria. From a stability point of view, the increasing or
700 constant value of the current peaks can be considered as an implicit indicator
701 of proper and developing exoelectrogenic activity [64].

702 In summary, based on the above discussion, it can be concluded that
703 anodes in both MFCs developed in a comparable way over time and the
704 involvement of (similar) endogenous redox mediators in accomplishing
705 mediated electron transfer can be supposed. Additionally, no limitation or
706 negative impact ascribed to the application of SILM appeared on the
707 electrochemical activity (relative to Nafion). However, further experiments will
708 be needed to study the membrane characteristics (e. g. swelling, stability,
709 resistance to biofouling, etc.) and their change over time, which are crucial
710 aspects of membrane development for bioelectrochemical applications [68], in
711 agreement with the implications made in the last paragraph of Section 3.1.
712

713 **3.7. Analysis of MFC internal resistance breakdown by electrochemical**
714 **impedance spectroscopy (EIS)**
715

716 The similar development of bioelectrochemical activity in the MFCs over
717 time was proved by the outcomes of biological and electrochemical process
718 characterization methods (Sections 3.5 and 3.6). EIS analysis is able to
719 provide more detailed insights to reveal how the total internal resistance of
720 MFC is influenced by the various factors. In fact, R_i can be considered as the
721 product of electrode (anode + cathode) charge transfer resistances (R_{CT}),
722 (solid + liquid) electrolyte (membrane + bulk solution) resistances (R_{M+S}) and
723 diffusion resistance (R_D), in accordance with Eq. 3.
724

$$R_i = R_{CT} + R_{M+S} + R_D \quad (3)$$

Therefore, complete fuel cell EIS spectra were registered in the MFCs (**Fig. 8**) at the 21th day of operation (last cycle appearing in **Fig, 2**). As it is also shown in **Fig. 8**, a symmetric equivalent circuit model – containing anodic and cathodic charge transfer resistances (R_{CT}), combined membrane/solution resistances (R_{M+S}), capacitances of the electrical double layer (C_{DL}) and a Warburg element (W) – was used to represent the experimental system, as suggested by Wei et al. [69]. By fitting this model to the data measured, R_{CT} and R_{M+S} could be obtained. As demonstrated by Nam et al. [70], once R_{CT} and R_{M+S} values are known, simple subtraction of those from R_i (according to Eq. 3) will lead to an estimate of the third resistance component, namely the diffusion resistance (R_D).

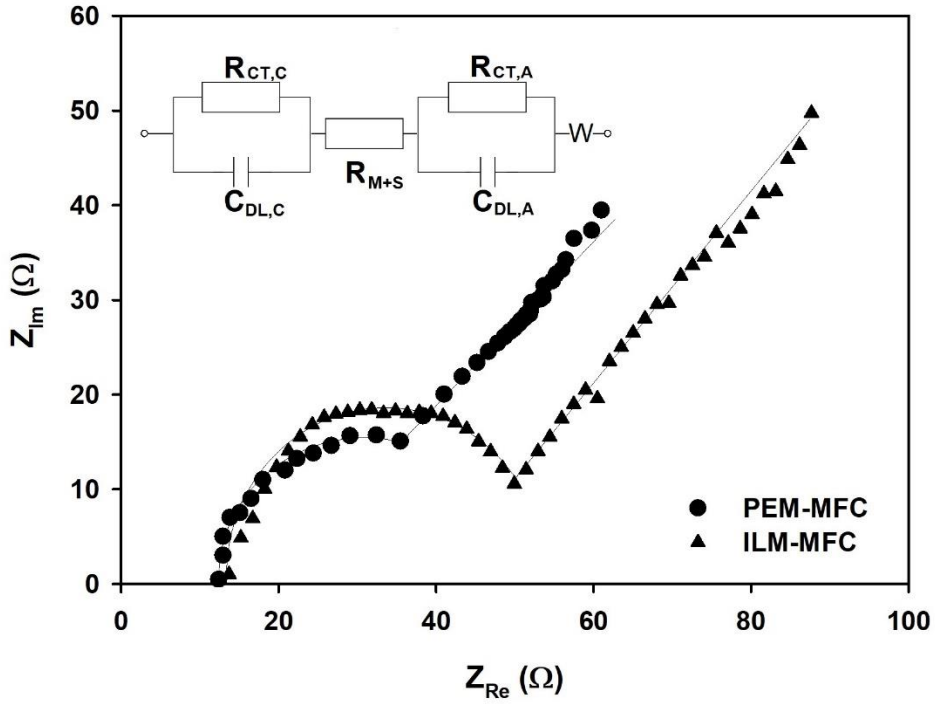

Fig. 8 – The whole-cell EIS spectra (Nyquist plots) for PEM-MFC and ILM-MFC (including experimental and model data) and the equivalent circuit model of the bioelectrochemical cells.

The results of model fitting and the resistance values calculated are listed in **Table 5**. As it can be seen, only slight differences in terms of R_{M+S} and R_{CT} could be noted in the MFCs regardless of the membrane type. Hence, as the results implied, the major difference could be observed for the diffusion resistances: in case of PEM-MFCs 253.9 Ω, while in ILM-MFCs 213.2 Ω were obtained. This means that in both systems, R_D had the highest contribution to the actual R_i (84 and 79 %, respectively).

Table 5 – Estimated values of different components of the total internal MFC resistance

MFC type	R_{CT} (Ω)	R_{M+S} (Ω)	R_D (Ω)	R_i (Ω)
PEM-MFC	35.7 ± 11.1	12.4 ± 1.9	253.9 ± 4	302 ± 17
ILM-MFC	41.1 ± 7.3	13.7 ± 0.9	213.2 ± 2.8	268 ± 11

These findings are in agreement with literature data [69-71], where diffusion resistance was frequently reported as the dominant factor affecting the total internal resistance. Diffusion resistance is connected to the slow diffusion of various chemical species present in MFC systems. The lower R_D in case of ILM-MFC could suggest that the transport of species involved in the cathodic reduction reaction and/or affecting the cathodic (electrode) environment was less performance limiting using the SILM as physical separator. As a result, this assumed phenomenon, to a certain extent, could lead to the reduction of mass transport limitations in ILM-MFC. On the contrary, these transport processes might be more hindered/less advantageous (relative to ILM-MFC) applying PEM. This assumption could support the findings of polarization measurements (described in Section 3.4) and the conclusions regarding **Fig. 6**, according to which the differences in the membrane-related mass transport processes (indicated by steady-state discrete cathode potential values) seemed to be a reasonable explanation behind the better performance of ILM-MFC. Nevertheless, further experiments

772 targeting the in-depth evaluation of mass transfer processes are needed for a
773 better understanding of the main differences between the transfer mechanisms
774 taking place through the PEMs and SILMs.
775
776 **4. Conclusions**
777
778 In this work, the effect of membrane separators on the performance and
779 behavior of microbial fuel cells was addressed. Various techniques such as
780 cyclic voltammetry, dehydrogenase enzyme activity measurement, cell
781 polarization, electrochemical impedance spectroscopy, estimation of both
782 Coulombic efficiency and energy recovery were applied for a comparative
783 assessment. It has turned out that membranes prepared with [bmim][PF_6] ionic
784 liquid and PVDF support matrix, depending on the conditions, could be
785 employed more efficiently than Nafion, the most commonly applied proton
786 exchange membrane. The main reason for better performance of the former
787 system seemed to be in relation with the differences of mass transfer
788 phenomena taking place through the IL-based membrane separator. During
789 the experiments, the use of SILM had no observable negative effect on the
790 biological catalysts of the MFCs, while it could potentially lead to reduced
791 mass transport limitations and thus, higher MFC efficiency. Therefore,
792 membranes made with ionic liquids can have the potential to be used as
793 attractive separators in bioelectrochemical systems such as MFCs.

Acknowledgements

The János Bolyai Research Scholarship of the Hungarian Academy of Sciences is duly acknowledged for the support. The “GINOP-2.3.2-15 – Excellence of strategic R+D workshops (Development of modular, mobile water treatment systems and waste water treatment technologies based on University of Pannonia to enhance growing dynamic export of Hungary (2016-2020))” is also thanked for supporting this work. Furthermore, this study was financially supported by “Fondo de Sustentabilidad Energética SENER – CONACYT (Mexico)”, through the project 247006 Gaseous Biofuels Cluster. László Koók was supported by the ÚNKP-17-3 ‘‘New National Excellence Program of the Ministry of Human Capacities”.

References

[1] B.E. Logan, B. Hamelers, R. Rozendal, U. Schröder, J. Keller, S. Freguia, et al., Microbial fuel cells: Methodology and technology, Environ. Sci. Technol. 40 (2006) 5181-5192.

[2] D. Pant, G. Van Bogaert, L. Diels, K. Vanbroekhoven, A review of the substrates used in microbial fuel cells (MFCs) for sustainable energy production, Bioresour. Technol. 101 (2010) 1533-1543.

[3] P. Pandey, V.N. Shinde, R.L. Deopurkar, S.P. Kale, S.A. Patil, D. Pant, Recent advances in the use of different substrates in microbial fuel cells toward wastewater treatment and simultaneous energy recovery, Appl. Energy 168 (2016) 706-723.

[4] J.M. Sonawane, S.B. Adeloju, P.C. Ghosh, Landfill leachate: A promising substrate for microbial fuel cells, Int. J. Hydrogen Energy 42 (2017) 23794-23798.

[5] G. Hernández-Flores, H.M. Poggi-Varaldo, T. Romero-Castañón, O. Solorza-Feria, N. Rinderknecht-Seijas, Harvesting energy from leachates

in microbial fuel cells using an anion exchange membrane, Int. J. Hydrogen Energy 42 (2017) 30374-30382.

[6] A. Colombo, A. Schievano, S.P. Trasatti, R. Morrone, N. D'Antona, P. Cristiani, Signal trends of microbial fuel cells fed with different food-industry residues, Int. J. Hydrogen Energy 42 (2017) 1841-1852.

[7] C. Lai, B. Li, M. Chen, G. Zeng, D. Huang, L. Qin, et al., Simultaneous degradation of P-nitroaniline and electricity generation by using a microfiltration membrane dual-chamber microbial fuel cell, Int J Hydrogen Energy 43 (2018) 1749-1757.

[8] D. Cecconet, D. Molognoni, A. Callegari, A.G. Capodaglio, Agro-food industry wastewater treatment with microbial fuel cells: Energetic recovery issues, Int. J. Hydrogen Energy 43 (2018) 500-511.

[9] S.T. Oh, J.R. Kim, G.C. Premier, T.H. Lee, C. Kim, W.T. Sloan, Sustainable wastewater treatment: How might microbial fuel cells contribute, Biotechnol. Adv. 28 (2010) 871-881.

[10] H. Hiegemann, D. Herzer, E. Nettmann, M. Lübken, P. Schulte, K.G. Schmelz, et al., An integrated 45 L pilot microbial fuel cell system at a full-scale wastewater treatment plant, Bioresour. Technol. 218 (2016) 115-222.

[11] R. Liu, H. Tursun, X. Hou, F. Odey, Y. Li, X. Wang, et al., Microbial community dynamics in a pilot-scale MFC-AA/O system treating domestic sewage, Bioresour. Technol. 241 (2017) 439-447.

[12] A. Escapa, M.I. San-Martín, R. Mateos, A. Morán, Scaling-up of membraneless microbial electrolysis cells (MECs) for domestic wastewater treatment: Bottlenecks and limitations, Bioresour. Technol. 180 (2015) 72-78.

[13] G. Kumar, P. Bakonyi, G. Zhen, P. Sivagurunathan, L. Koók, S.H. Kim, et al., Microbial electrochemical systems for sustainable biohydrogen production: Surveying the experiences from a start-up viewpoint, Renew. Sustain. Energy Rev. 70 (2017) 589-597.

[14] C. Santoro, S. Rojas-Carbonell, R. Awais, R. Gokhale, M. Kodali, A. Serov, et al., Influence of platinum group metal-free catalyst synthesis on microbial fuel cell performance, J. Power Sources 375 (2018) 11-20.

[15] W.W. Li, G.P. Sheng, X.W. Liu, H.Q. Yu, Recent advances in the separators for microbial fuel cells, Bioresour. Technol. 102 (2011) 244-252.

[16] H. Zhang, S. Cheng, X. Wang, X. Huang, B.E. Logan, Separator characteristics for increasing performance of microbial fuel cells, Environ. Sci. Technol. 43 (2009) 8456-8461.

[17] M. Oliot, S. Galier, H. Roux de Balmann, A. Bergel, Ion transport in microbial fuel cells: Key roles, theory and critical review, Appl. Energy 183 (2016) 1682-1704.

[18] B.R. Dhar, H.S. Lee, Membranes for bioelectrochemical systems: challenges and research advances, Environ. Technol. 34 (2013) 1751-1764.

[19] T.H.J.A. Sleutels, A. ter Heijne, P. Kuntke, C.J.N. Buisman, H.V.M. Hamelers, Membrane selectivity determines energetic losses for ion transport in bioelectrochemical systems, ChemistrySelect 2 (2017) 3462-3470.

[20] M. Rahimnejad, G. Bakeri, M. Ghasemi, A. Zirepour, A review on the role of proton exchange membrane on the performance of microbial fuel cell, Polym. Adv. Technol. 25 (2014) 1426-1432.

[21] K.J. Chae, M. Choi, F.F. Ajayi, W. Park, I.S. Chang, I.S. Kim, Mass transport through a proton exchange membrane (Nafion) in microbial fuel cells, Energy Fuels 22 (2008)169-176.

[22] K.Y. Kim, K.J. Chae, M.J. Choi, E.T. Yang, M.H. Hwang, I.S. Kim, High-quality effluent and electricity production from non-CEM based flow-through type microbial fuel cell, Chem. Eng. J. 218 (2013) 19-23.

[23] S.E. Oh, B.E. Logan, Proton exchange membrane and electrode surface areas as factors that affect power generation in microbial fuel cells, Appl. Microbiol. Biotechnol. 70 (2006) 162-169.

[24] S. Angioni, L. Millia, G. Bruni, C. Tealdi, P. Mustarelli, E. Quartarone, Improving the performances of Nafion™-based membranes for microbial fuel cells with silica-based, organically-functionalized mesostructured fillers, J. Power Sources 334 (2016) 120-127.

[25] J.R. Kim, S. Cheng, S.E. Oh, B.E. Logan, Power generation using different cation, anion, and ultrafiltration membranes in microbial fuel cells, Environ. Sci. Technol. 41 (2007) 1004-1009.

[26] V. Kumar, R. Rudra, A. Nandy, S. Hait, P.P. Kundu, Analysis of partially sulfonated low density polyethylene (LDPE) membranes as separators in microbial fuel cells, RSC Adv. 7 (2017) 21890-21900.

[27] X. Tang, K. Guo, H. Li, Z. Du, J. Tian, Microfiltration membrane performance in two-chamber microbial fuel cells, Biochem. Eng. J. 52 (2010) 194-198.

[28] E. Yang, K.J. Chae, I.S. Kim, Assessment of different ceramic filtration membranes as a separator in microbial fuel cells, Desalin. Water Treat. 57 (2016) 28077-28085.

[29] J. Winfield, I. Gajda, J. Greenman, I. Ieropoulos, A review into the use of ceramics in microbial fuel cells, Bioresour. Technol. 215 (2016) 296-303.

[30] D. Pant, G. Van Bogaert, Y. Alvarez-Gallego, L. Diels, K. Vanbroekhoven, Evaluation of bioelectrogenic potential of four industrial effluents as substrate for low cost Microbial Fuel Cells operation, Environ. Eng. Manag. J. 51 (2016) 1897-1904.

[31] A.S. Mathuriya, D. Pant, Assessment of expanded polystryrene as a separator in microbial fuel cell, Environ. Technol. (2018), doi: https://doi.org/10.1080/09593330.2018.1435740

[32] F.J. Hernández-Fernández, A.P. de los Ríos, F. Mateo-Ramirez, C. Godínez, L.J. Lozano-Blanco, J.I. Moreno, et al., New application of supported ionic liquids membranes as proton exchange membranes in microbial fuel cell for waste water treatment, Chem. Eng. J. 279 (2015) 115-119.

[33] L. Koók, N. Nemestóthy, P. Bakonyi, G. Zhen, G. Kumar, X. Lu, et al., Performance evaluation of microbial electrochemical systems operated with Nafion and supported ionic liquid membranes, Chemosphere 175 (2017) 350-355.

[34] L. Koók, N. Nemestóthy, P. Bakonyi, A. Göllei, T. Rózsenberszki, P. Takács, et al., On the efficiency of dual-chamber biocatalytic electrochemical cells applying membrane separators prepared with imidazolium-type ionic liquids containing $[NTf_2]^-$ and $[PF_6]^-$ anions, Chem. Eng. J. 324 (2017) 296-302.

[35] P. Bakonyi, L. Koók, E. Keller, K. Bélafi-Bakó, T. Rózsenberszki, G.D. Saratale, et al., Development of bioelectrochemical systems using various biogas fermenter effluents as inocula and municipal waste liquor as adapting substrate, Bioresour. Technol. 259 (2018)75-82.

[36] M. Ghasemi, W.R.W. Daud, M. Ismail, M. Rahimnejad, A.F. Ismail, J.X. Leong, et al., Effect of pre-treatment and biofouling of proton exchange membrane on microbial fuel cell performance, Int. J. Hydrogen Energy 38 (2013) 5480-5484.

[37] L.E. Casida, D.A. Klein, T. Santoro, Soil dehydrogenase activity, Soil Science 98 (1964) 371-376.

[38] M.V. Reddy, S. Srikanth, S.V. Mohan, P.N. Sarma, Phosphatase and dehydrogenase activities in anodic chamber of single chamber microbial fuel cell (MFC) at variable substrate loading conditions, Bioelectrochemistry 77 (2010) 125-132.

[39] J. Wang, J. Luo, S. Feng, H. Li, Y. Wan, X. Zhang, Recent development of ionic liquid membranes, Green Energy Environ. 1 (2016) 43-61.

[40] R. Fortunato, C.A.M. Afonso, J. Benavente, E. Rodriguez-Castellón, J.G. Crespo, Stability of supported ionic liquid membranes as studied by X-ray photoelectron spectroscopy, J. Membr. Sci. 256 (2005) 216-223.

[41] P. Wasserscheid, T. Welton, Ionic liquids in synthesis, John Wiley & Sons, 2008.

[42] R. Fortunato, C.A.M. Afonso, M.A.M. Reis, J.G. Crespo, Supported liquid membranes using ionic liquids: study of stability and transport mechanisms, J. Membr. Sci. 242 (2004) 197-209.

[43] N. Nemestóthy, P. Bakonyi, T. Rózsenberszki, G. Kumar, L. Koók, G. Kelemen, et al., Assessment via the modified gompertz-model reveals new insights concerning the effects of ionic liquids on biohydrogen production, Int. J. Hydrogen Energy 43 (2018) 18918-18924.

[44] M. Jebur, A. Sengupta, Y.H. Chiao, M. Kamaz, X. Qian, R. Wickramasinghe, Pi electron cloud mediated separation of aromatics using supported ionic liquid (SIL) membrane having antibacterial activity, J. Membr. Sci. 556 (2018) 1-11.

[45] S. Roy, A. Schievano, D. Pant, Electro-stimulated microbial factory for value added product synthesis, Bioresour. Technol. 213 (2016) 129-139.

[46] H. Liu, S. Cheng, B.E. Logan, Production of electricity from acetate or butyrate using a single-chamber microbial fuel cell, Environ. Sci. Technol. 39 (2005) 658-662.

[47] T.H.J.A. Sleutels, L. Darus, H.V.M. Hamelers, C.J.N. Buisman, Effect of operational parameters on Coulombic efficiency in bioelectrochemical systems, Bioresour. Technol. 102 (2011) 11172-11176.

[48] S.V. Raghavulu, S.V. Mohan, R.K. Goud, P.N. Sarma. Effect of anodic pH microenvironment on microbial fuel cell (MFC) performance in concurrence with aerated and ferricyanide catholytes, Electrochem. Commun. 11 (2009) 371-375.

[49] S.V. Mohan, R. Saravanan, S.V. Raghavulu, G. Mohanakrishna, P.N. Sarma, Bioelectricity production from wastewater treatment in dual chambered microbial fuel cell (MFC) using selectively enriched mixed microflora: effect of catholyte, Bioresour. Technol. 99 (2008) 596-603.

977 [50] P. Bakonyi, L. Koók, G. Kumar, G. Tóth, T. Rózsenberszki, D.D.
978 Nguyen, et al., Architectural engineering of bioelectrochemical systems
979 from the perspective of polymeric membrane separators: A
980 comprehensive update on recent progress and future prospects, J.
981 Membr. Sci. 564 (2018) 508-522.
982 [51] Z. Ge, J. Li, L. Xiao, Y. Tong, Z. He, Recovery of electrical energy
983 in microbial fuel cells, Environ. Sci. Technol. Lett. 1 (2014) 137-141.
984 [52] J. Li, H. Li, J. Zheng, L. Zhang, Q. Fu, X. Zhu, et al., Response of
985 anodic biofilm and the performance of microbial fuel cells to different
986 discharging current densities, Bioresour. Technol. 233 (2017) 1-6.
987 [53] S.V. Mohan, G. Mohanakrishna, S. Srikanth, P.N. Sarma,
988 Harnessing of bioelectricity in microbial fuel cell (MFC) employing
989 aerated cathode through anaerobic treatment of chemical wastewater
990 using selectively enriched hydrogen producing mixed consortia, Fuel 87
991 (2008) 2667-2676.
992 [54] F.J. Hernández-Fernández, A.P. de los Ríos, F. Mateo-Ramírez,
993 M.D. Juarez, L.J. Lozano-Blanco, C. Godínez, New application of
994 polymer inclusion membrane based on ionic liquids as proton exchange
995 membrane in microbial fuel cell, Sep. Purif. Technol. 160 (2016) 51-58.
996 [55] R.A. Rozendal, H.V.M. Hamelers, C.J.N. Buisman, Effects of
997 membrane cation transport on pH and microbial fuel cell performance,
998 Environ. Sci. Technol. 40 (2006) 5206-5211.
999 [56] F. Harnisch, U. Schröder, F. Scholz, The suitability of monopolar
1000 and bipolar ion exchange membranes as separators for biological fuel
1001 cells, Environ. Sci. Technol. 42 (2008) 1740-1746.
1002 [57] H. Rismani-Yazdia, S.M. Carver, A.D. Christy, O.H. Tuovinen,
1003 Cathodic limitations in microbial fuel cells: An overview, J. Power
1004 Sources 180 (2008) 683-694.
1005 [58] B.E. Logan, Exoelectrogenic bacteria that power microbial fuel
1006 cells, Nature Rev. Microbiol. 7 (2009) 375-381.

[59] A.P. Borole, C.Y. Hamilton, T. Vishnivetskaya, D. Leak, C. Andras, Improving power production in acetate-fed microbial fuel cells via enrichment of exoelectrogenic organisms in flow-through systems, Biochem. Eng. J. 48 (2009) 71-80.

[60] H.S. Park, B.H. Kim, H.S. Kim, H.J. Kim, G.T. Kim, M. Kim, et al., A novel electrochemically active and Fe (III)-reducing bacterium phylogenetically related to Clostridium butyricum isolated from a microbial fuel cell, Anaerobe 7 (2001) 297-306.

[61] K. Rabaey, N. Boon, S.D. Siciliano, M. Verhaege, W. Verstraete, Biofuel cells select for microbial consortia that self-mediate electron transfer, Appl. Environ. Microbiol. 70 (2004) 5373-5382.

[62] S.V. Mohan, S.V. Raghavulu, P.N. Sarma, Influence of anodic biofilm growth on bioelectricity production in single chambered mediatorless microbial fuel cell using mixed anaerobic consortia, Biosen. Bioelectron. 24 (2008) 41-47.

[63] S.A. Patil, F. Harnisch, B. Kapadnis, U. Schröder, Electroactive mixed culture biofilms in microbial bioelectrochemical systems: the role of temperature for biofilm formation and performance, Biosens. Bioelectron. 26 (2010) 803-808.

[64] F. Harnisch, S. Freguia, A basic tutorial on cyclic voltammetry for the investigation of electroactive microbial biofilms, Chem. Asian J. 7 (2012) 466-475.

[65] A.J. Bard, L.R. Faulkner, Electrochemical methods: Fundamentals and applications, 2nd edition, John Wiley & Sons, Inc., 2001.

[66] J. Babauta, R. Renslow, Z. Lewandowski, H. Beyenal, Electrochemically active biofilms: facts and fiction. A review, Biofouling 28 (2012) 789-812.

[67] S.B. Velasquez-Orta, I.M. Head, T.P. Curtis, K. Scott, Factors affecting current production in microbial fuel cells using different industrial wastewaters, Bioresour. Technol. 102 (2011) 5105-5112.

[68] J.R. Varcoe, P. Atanassov, D.R. Dekel, A.M. Herring, M.A. Hickner, P.A. Kohl, et al., Anion-exchange membranes in electrochemical energy systems, Energy Environ. Sci. 7 (2014) 3135-3191.

[69] B. Wei, J.C. Tokash, F. Zhang, Y. Kim, B.E. Logan, Electrochemical analysis of separators used in single-chamber, air-cathode microbial fuel cells, Electrochim. Acta 89 (2013) 45-51.

[70] J.Y. Nam, H.W. Kim, K.H. Lim, H.S. Shin, B.E. Logan, Variation of power generation at different buffer types and conductivities in single chamber microbial fuel cells, Biosens. Bioelectron. 25 (2010) 1155-1159.

[71] A.J. Hutchinson, J.C. Tokash, B.E. Logan, Analysis of carbon fiber brush loading in anodes on startup and performance of microbial fuel cells, J. Power Sources 196 (2011) 9213-9219.